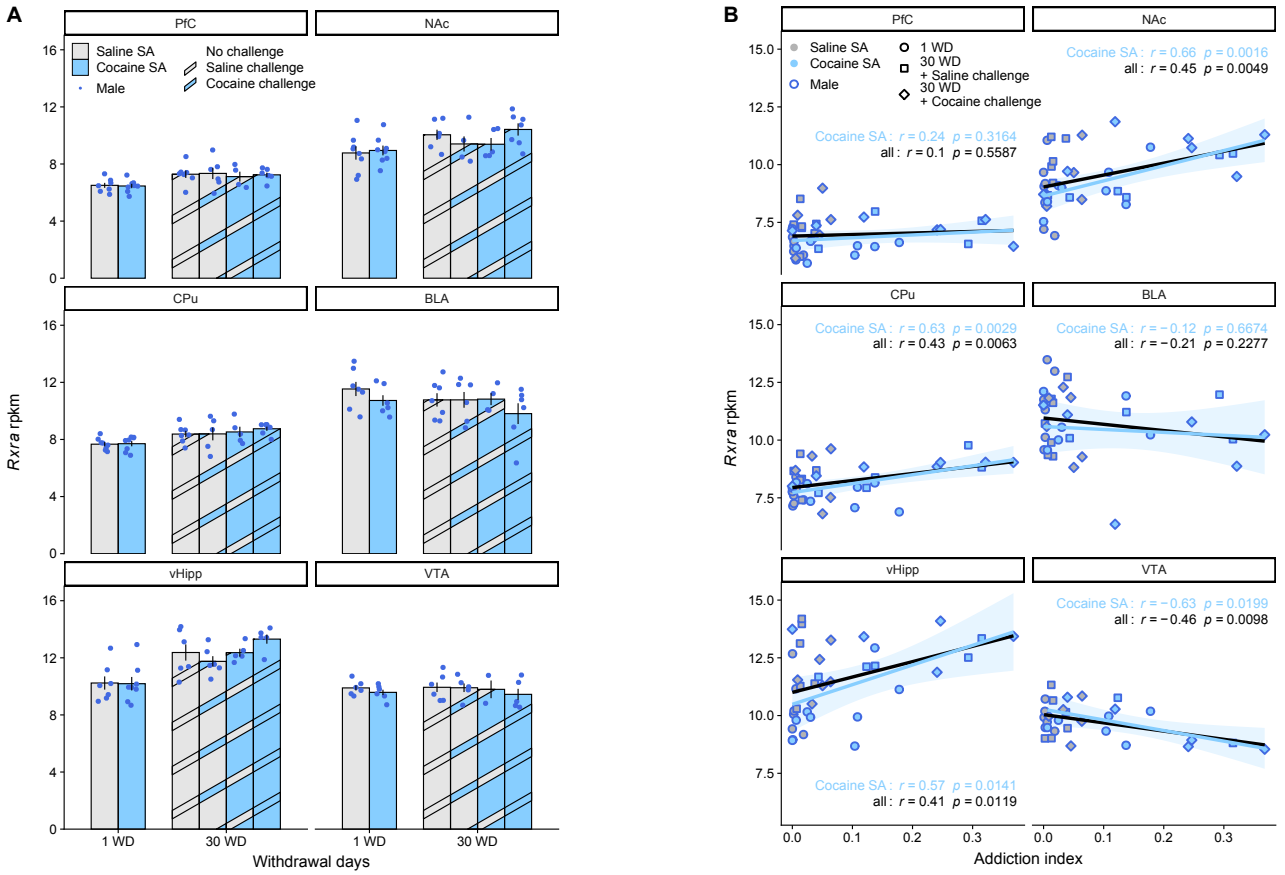

Figure S1. Brain-wide RXRα expression after cocaine self-administration. *(related to Figure 1)*

(A) RNAseq of bulk NAc tissue showed no regulation of *Rxra* transcripts across experimental groups in any of the six brain regions analyzed (data from original study [11]).

(B) Correlation between *Rxra* levels and the Addiction Index, a composite metric representative of addiction-like behavioral domains computed using exploratory factor analysis [11] was positive in NAc (across all samples: Pearson's r = 0.45, p = 0.0049; across cocaine SA samples only: Pearson's r = 0.66, p = 0.0016), CPu (across all samples: Pearson's r = 0.43, p = 0.0063; across cocaine SA samples only: Pearson's r = 0.63, p = 0.0029) and vHipp (across all samples: Pearson's r = 0.41, p = 0.0119; across cocaine SA samples only: Pearson's r = 0.57, p = 0.0141) and negative in VTA (across all samples: Pearson's r = -0.46, p = 0.0098; across cocaine SA samples only: Pearson's r = -0.63, p = 0.0199).

Bar graphs represent mean ± sem. Correlation graphs represent regression line with its 95% confidence interval.

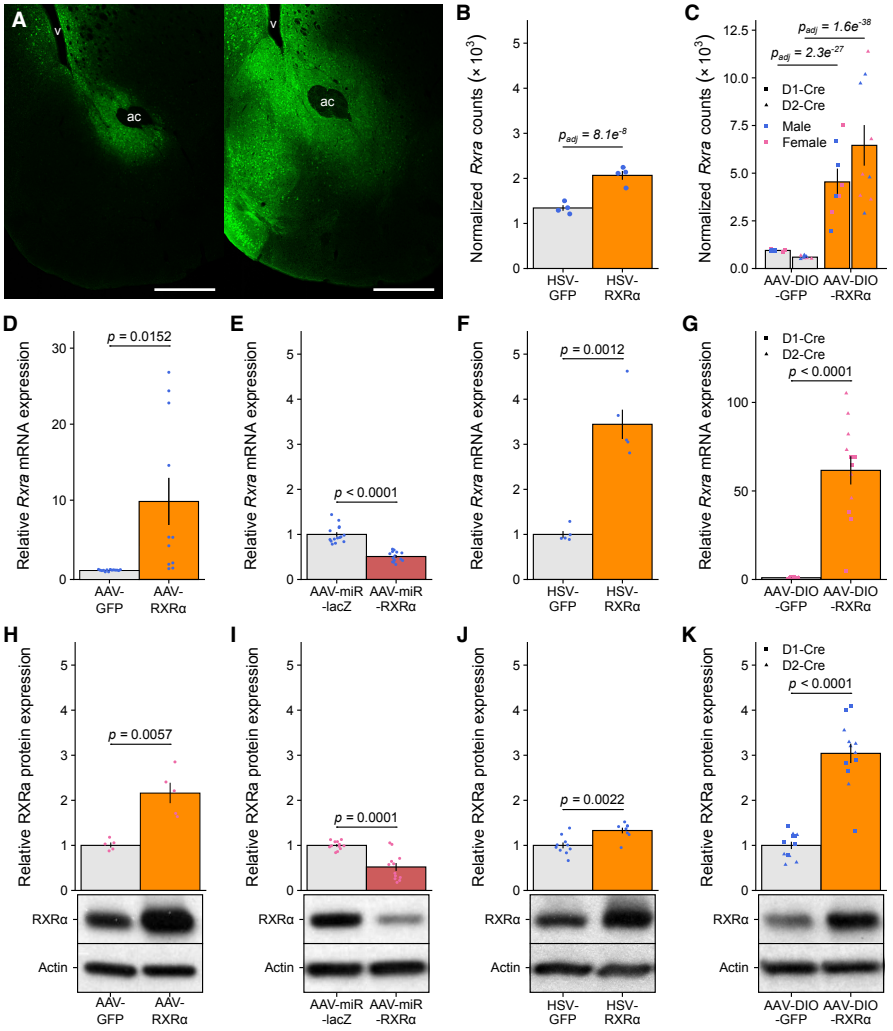

Figure S2. Validation of viral constructs. *(related to Figures 1, 3, 4, 5 and 6)*

(A) Representative images of viral infusions targeting the anterior NAc core for HSV (left) and AAV (right) viruses, picturing maximal levels of viral spread in tissue. HSV infection was restricted to NAc core, while AAV infections spread to NAc core and medial shell. Backflow infection was observed ~20% of the time along both sides of the lateral ventricles, as shown in these representative images, but the presence of such backflow did not affect results of the experiments. ac anterior commissure, v lateral ventricle. Scale bars represent 500 µm.

(B) NAc *Rxra* transcripts count was significantly increased in male wild type mice injected with HSV-RXRα via RNAseq (Figure 1 dataset; Wald's test, $p_{adj} = 8.1e^{-8}$).

(C) *Rxra* transcript counts were significantly increased in D1-MSNs from male and female D1-Cre x $^{fl/fl}$eGFP::L10a mice (Figure 3 dataset; Wald's test, $p_{adj} = 2.3e^{-27}$) and in D2-MSNs from male and female D2-Cre x $^{fl/fl}$eGFP::L10a mice sorting (Figure 4 dataset; Wald's test, $p_{adj} = 1.6e^{-38}$) injected with AAV-DIO-RXRα via RNAseq after FAN-sorting.

(D) NAc *Rxra* transcript levels were significantly increased in male wild type mice injected with AAV-RXRα via RT-qPCR (unpaired Welch's *t*-test: $t_{10.003} = -2.923$, $p = 0.01522$).

(E) NAc *Rxra* transcripts levels were significantly decreased in male wild type mice injected with AAV-miR-RXRα via RT-qPCR (unpaired Welch's *t*-test: $t_{22.58} = 8.4543$, $p = 1.899e^{-8}$).

(F) NAc *Rxra* transcripts levels were significantly increased in male wild type mice injected with HSV-RXRα via RT-qPCR (unpaired Welch's *t*-test: $t_{4.4178} = -7.3332$, $p = 0.00124$).

(G) NAc *Rxra* transcripts levels were significantly increased in female D1-Cre and D2-Cre mice injected with AAV-DIO-RXRα via RT-qPCR (LMM-ANOVA: main effect of Virus: $F_{1,20} = 77.2889$, $p = 1.559e^{-8}$, followed by Sidak's *post hoc* tests).

(H) NAc RXRα protein levels were significantly increased in female wild type mice injected with HSV-RXRα via Western blotting (unpaired Welch's *t*-test: $t_{4.4893} = -4.9468$, $p = 0.005747$).

(I) NAc RXRα protein levels were significantly increased in male wild type mice injected with HSV-RXRα via Western Blot (unpaired Welch's *t*-test: $t_{15.847} = 3.6574$, $p = 0.002155$).

(J) NAc RXRα protein levels were significantly decreased in female wild type mice injected with AAV-miR-RXRα via Western Blot (unpaired Welch's *t*-test: $t_{13.186} = 5.2867$, $p = 0.0001404$).

(K) NAc RXRα protein levels were significantly decreased in male D1-Cre and D2-Cre mice injected with AAV-DIO-RXRα via Western Blot (LMM-ANOVA: main effect of Virus: $F_{1,20} = 74.8156$, $p = 3.418e^{-8}$, followed by Sidak's *post hoc* tests).

Representative Western Blot pictures for RXRα and control actin bands are attached to the corresponding quantification. Bar graphs represent mean ± sem.

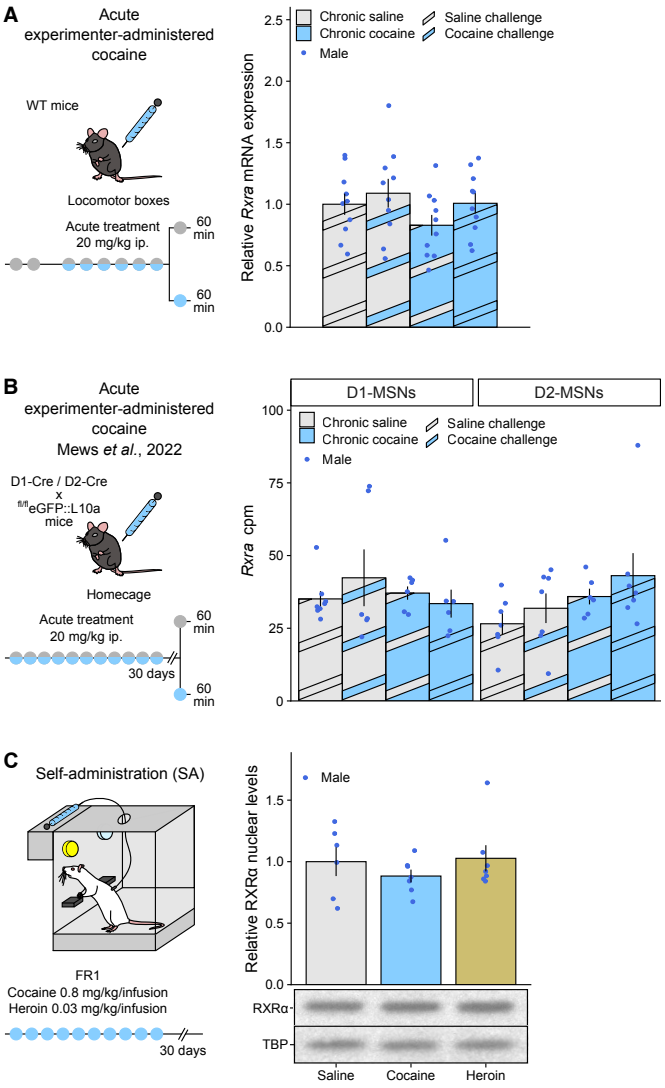

Figure S3. RXRα expression after chronic drug exposure. *(related to Figures 2 and 3)*

(A) NAc *Rxra* transcripts levels were not significantly regulated in male wild type mice after 6 days of chronic cocaine and 60 min after a cocaine challenge or not (LMM-ANOVA: main effect of Chronic: $F_{1,36} = 1.8299$, $p = 0.1846$, main effect of Challenge: $F_{1,36} = 2.0562$, $p = 0.1602$, interaction Chronic:Challenge: $F_{1,36} = 0.2277$, $p = 0.6361$, followed by Sidak's *post hoc* tests).

(B) *Rxra* transcripts counts were not significantly regulated in either sorted D1- or D2-MSNs from male D1-Cre or D2-Cre x $^{fl/fl}$eGFP::L10a mice after 10 days of chronic cocaine and 60 min after a cocaine challenge injection 30 days later (original data from [41]), reanalyzed by LMM-ANOVA, full statistics in Supplemental Table S6)

(C) NAc RXRα nuclear levels were not significantly regulated after 30 days of withdrawal from cocaine or heroin self-administration in male rats (LMM-ANOVA: main effect of Drug: $F_{2,17} = 0.6878$, $p = 0.5161$)

Representative Western Blot pictures for RXRα and control TBP bands are attached to the corresponding quantification. Bar graphs represent mean ± sem.

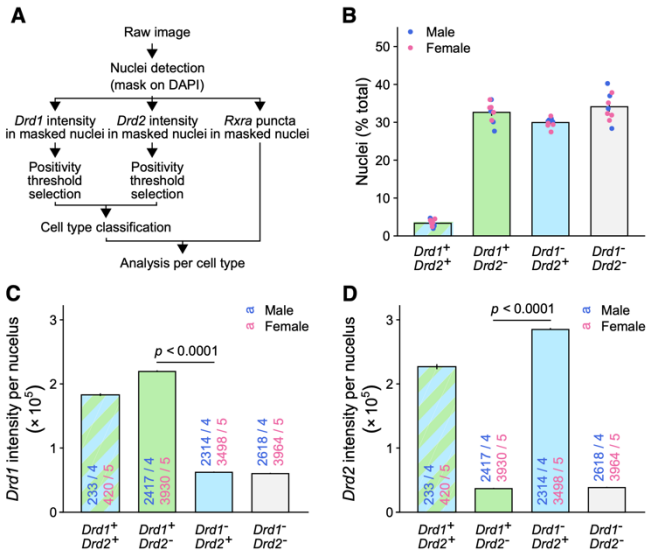

Figure S4. RNA FISH-based classification of NAc cell types. *(related to Figure 3)*

(A) Schematic pipeline for RNA FISH image analysis, cell type classification and signal quantification.

(B) Detected and classified cell types recapitulated expected relative abundance in mouse NAc (LMM-ANOVA: main effect of CellType: $F_{3,28} = 291.6805$, $p < 2e^{-16}$, followed by Sidak's *post hoc* tests).

(C) *Drd1* expression across NAc cell types (LMM-ANOVA: main effect of CellType: $F_{3,19381.2} = 16327.88$, $p < 2e^{-16}$, followed by Sidak's *post hoc* tests).

(D) *Drd2* expression across NAc cell types (LMM-ANOVA: main effect of CellType: $F_{3,19380.4} = 21539.97$, $p < 2e^{-16}$, followed by Sidak's *post hoc* tests).

Bar graphs represent mean ± sem after combining male and female data.

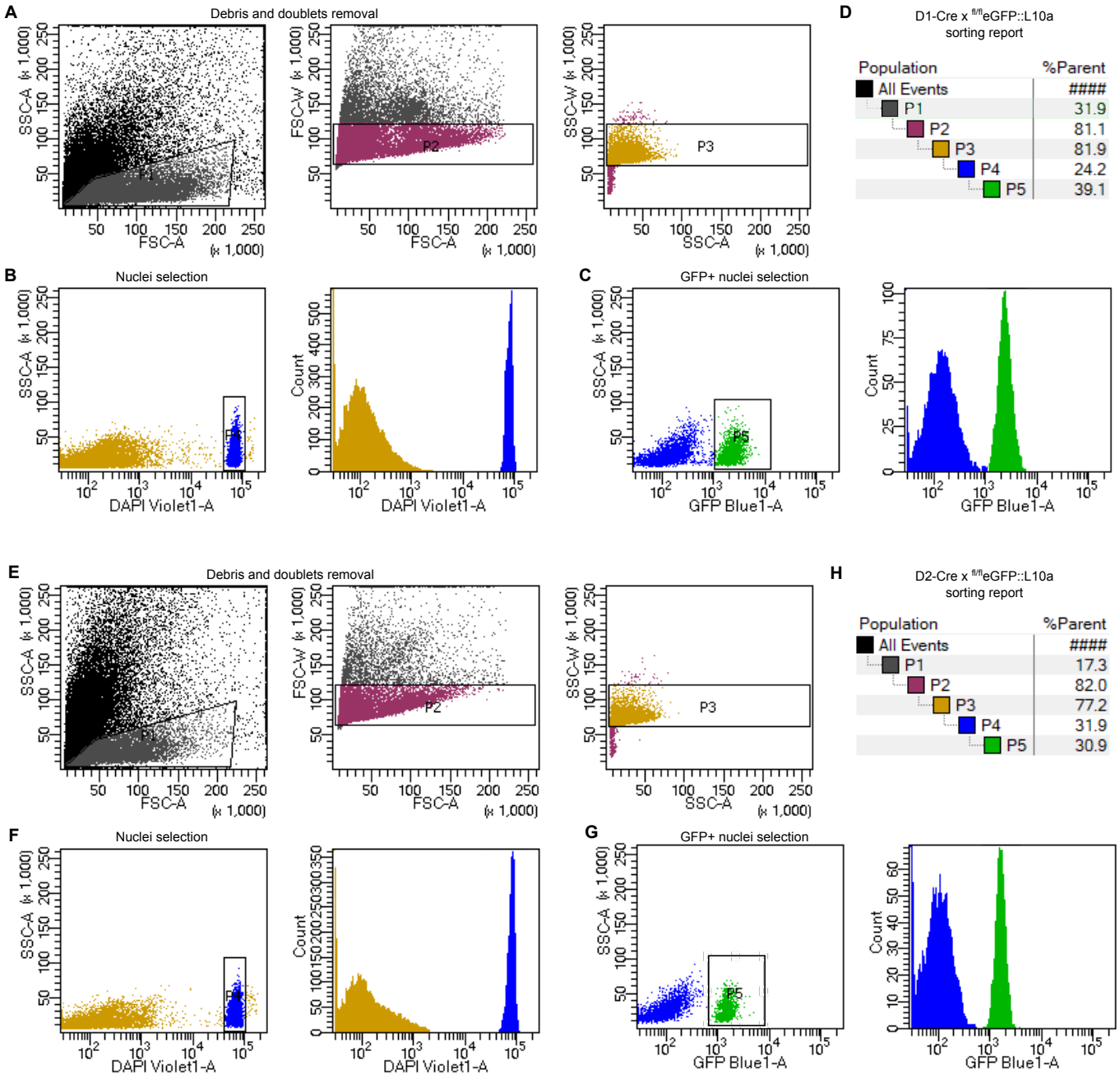

Figure S5. FAN-sorting of nuclei from D1- and D2-MSNs. *(related to Figure 3)*

(A) Representative FANS gating strategy to exclude debris and doublets from a D1-Cre x $^{fl/fl}$eGFP::L10a sample.

(B) Representative FANS gating strategy to select nuclei (*ie* DAPI+ events) from a D1-Cre x $^{fl/fl}$eGFP::L10a sample.

(C) Representative FANS gating strategy to select D1-MSNs nuclei (*ie* GFP+ events) from a D1-Cre x $^{fl/fl}$eGFP::L10a sample.

(D) Summary of FAN-sorting hierarchical gating strategy for a D1-Cre x $^{fl/fl}$eGFP::L10a sample.

(E) Representative FANS gating strategy to exclude debris and doublets from a D2-Cre x $^{fl/fl}$eGFP::L10a sample.

(F) Representative FANS gating strategy to select nuclei (*ie* DAPI+ events) from a D2-Cre x $^{fl/fl}$eGFP::L10a sample.

(G) Representative FANS gating strategy to select D2-MSNs nuclei (*ie* GFP+ events) from a D2-Cre x $^{fl/fl}$eGFP::L10a sample.

(H) Summary of FAN-sorting hierarchical gating strategy for a D2-Cre x $^{fl/fl}$eGFP::L10a sample.

FSC = Forward Scatter, SSC = Side Scatter.

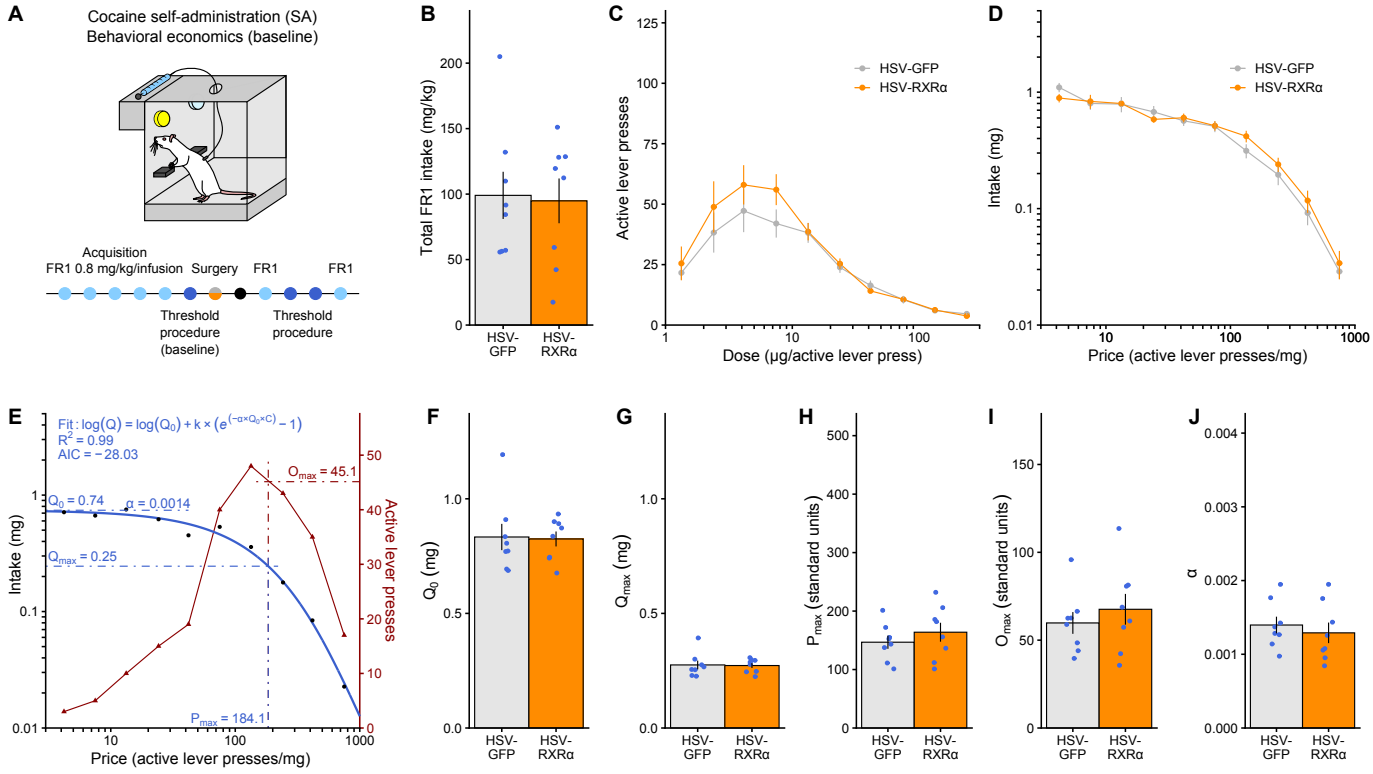

Figure S6. Behavioral economics metrics before RXRα overexpression. *(related to Figure 6)*

(A) Experimental design for behavioral economics testing, using male rats (n = 8/group). Before surgery, animals went through the threshold procedure to assess motivation at baseline, which is described here.

(B) Total cocaine intake in acquisition FR1 sessions was similar before group assignment (unpaired Welch's *t*-test: $t_{13.961} = 0.16909$, $p = 0.8682$).

(C) Dose response curves in the threshold procedure showed similar responding before group assignment (LMM-ANOVA: interaction Dose:Virus: $F_{9,126} = 0.7509$, $p = 0.6617$, followed by Sidak's *post hoc* tests).

(D) Averaged demand curves were also similar before group assignment (LMM-ANOVA: interaction Price:Virus: $F_{9,126} = 0.9386$, $p = 0.4943$, followed by Sidak's *post hoc* tests).

(E) Representative example of task performance in the threshold procedure at baseline (from a rat later injected with HSV-GFP control), highlighting mathematical demand curve fitting and extraction of behavioral economics parameters. Goodness of fit was assessed by computing a pseudo-R^2 coefficient and the Akaike Information Criterion (AIC) for each individual fit.

(F) Consumption at low effort Q_0 (unpaired Welch's *t*-test: $t_{11.098} = 0.12458$, $p = 0.9031$),

(G) consumption at maximum effort Q_{max} (unpaired Welch's *t*-test: $t_{11.016} = 0.13065$, $p = 0.8984$),

(H) P_{max} (unpaired Welch's *t*-test: $t_{12.512} = -0.87304$, $p = 0.3991$),

(I) O_{max} (unpaired Welch's *t*-test: $t_{12.601} = -0.72455$, $p = 0.482$) and

(J) demand elasticity α (unpaired Welch's *t*-test: $t_{13.426} = 0.58991$, $p = 0.5651$) were similar before group assignment.

Bar graphs and line graphs represent mean ± sem.

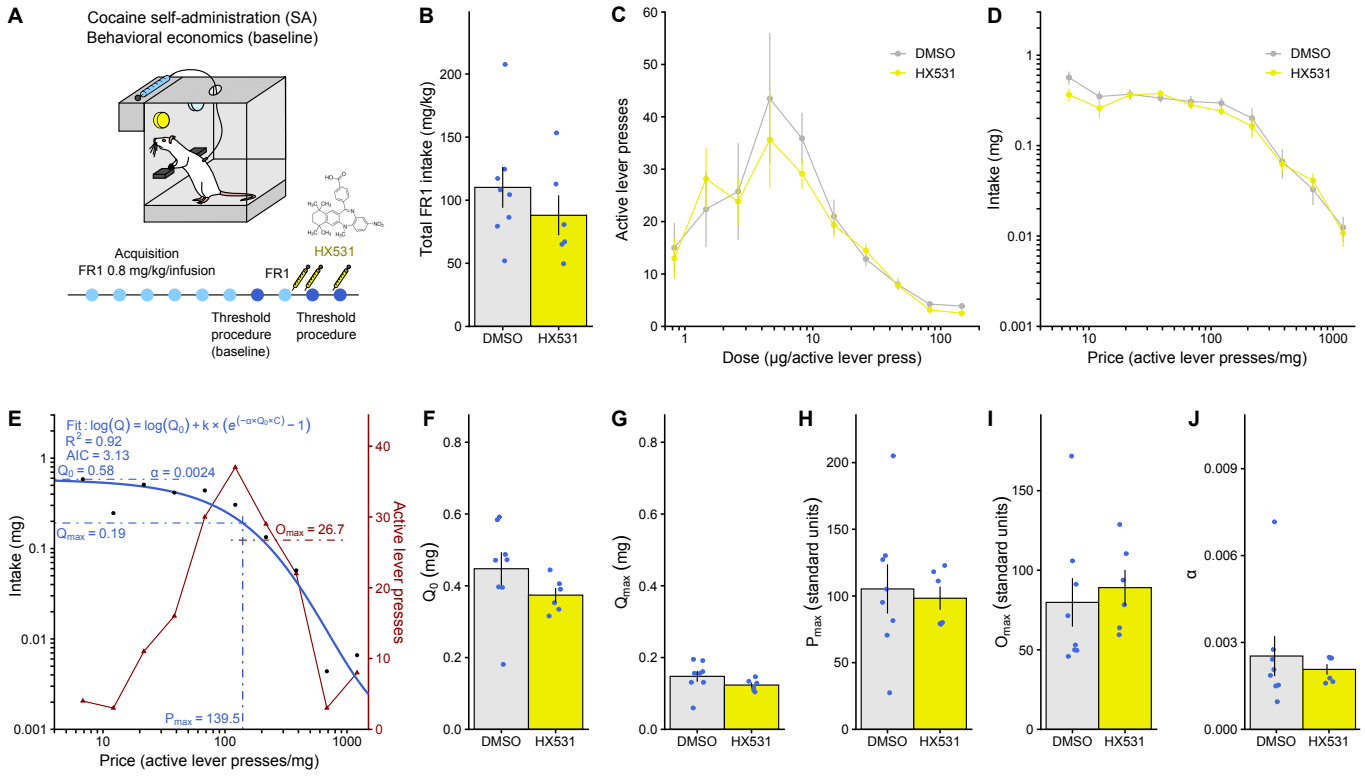

Figure S7. Behavioral economics metrics before HX531 treatment. *(related to Figure 7)*

(A) Experimental design for behavioral economics testing, using male rats (n = 6-8/group). Before group allocation, animals went through the threshold procedure to assess motivation at baseline, which is described here.

(B) Total cocaine intake in acquisition FR1 sessions was similar before group assignment (unpaired Welch's *t*-test: $t_{11.753} = 0.97974$, $p = 0.347$).

(C) Dose response curves in the threshold procedure showed similar responding before group assignment (LMM-ANOVA: interaction Dose:Treatment: $F_{9,108} = 0.3064$, $p = 0.9713$, followed by Sidak's *post hoc* tests).

(D) Averaged demand curves were also similar before group assignment (LMM-ANOVA: interaction Price:Treatment: $F_{9,108} = 1.3182$, $p = 0.2359$, followed by Sidak's *post hoc* tests).

(E) Representative example of task performance in the threshold procedure at baseline (from a rat later treated with DMSO), highlighting mathematical demand curve fitting and extraction of behavioral economics parameters. Goodness of fit was assessed by computing a pseudo-R^2 coefficient and the Akaike Information Criterion (AIC) for each individual fit.

(F) Consumption at low effort Q_0 (unpaired Welch's *t*-test: $t_{9.3667} = 1.4658$, $p = 0.1754$) was similar before group assignment.

(G) Consumption at maximum effort Q_{max} (unpaired Welch's *t*-test: $t_{9.353} = 1.4754$, $p = 0.173$) was also similar.

(H) P_{max} (unpaired Welch's *t*-test: $t_{9.769} = 0.34296$, $p = 0.7389$) was also similar.

(I) O_{max} (unpaired Welch's *t*-test: $t_{11.761} = -0.49087$, $p = 0.6325$) was also similar.

(J) Demand elasticity α (unpaired Welch's *t*-test: $t_{7.9396} = 0.64455$, $p = 0.5374$) was also similar.

Bar graphs and line graphs represent mean ± sem.

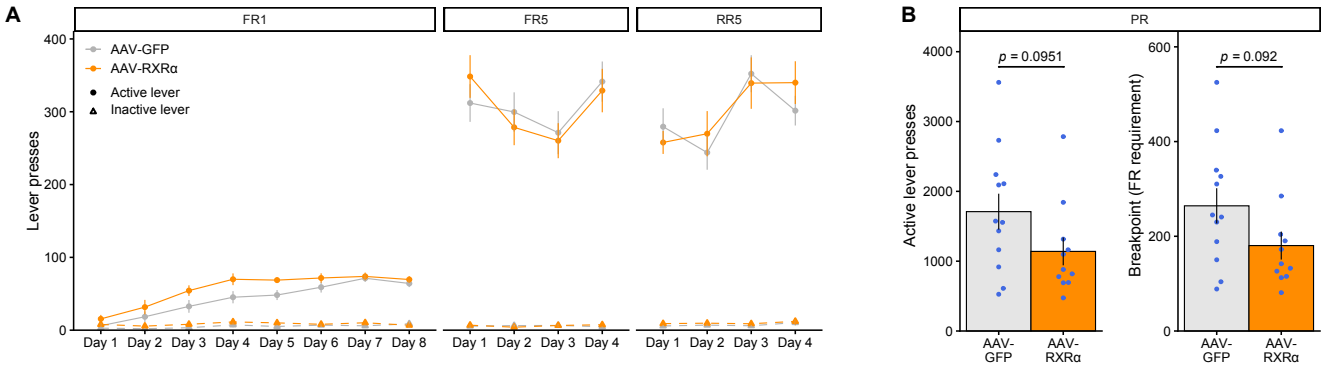

Figure S8. Lever pressing behavior during saccharine water operant responding. *(related to Figure 8)*

(A) Lever pressing behavior during FR1 acquisition and stable responding under FR5 and RR5 schedules (full statistics in Supplemental Table S6)

(B) Motivation-related parameters under PR schedule. RXRα overexpression resulted in trending decreases in total number of active lever presses (left, unpaired Welch's *t*-test: $t_{20.187} = 1.7512$, $p = 0.0951$) and in breakpoint measured as the last FR requirement reached and failed (right, unpaired Welch's *t*-test: $t_{20.353} = 1.7682$, $p = 0.09202$), both averaged across 3 consecutive testing days.

Bar graphs and line graphs represent mean ± sem.

Gene	Forward (5' to 3')	Reverse (5' to 3')
Arc	GGAGGGAGGTCTTCTACCGT	CTACAGAGACAGTGTGGCGG
Drd1a	TTCTTCCTGGTATGGCTTGG	GCTTAGCCCTCACGTTCTTG
Drd2	TATGCCCTGGGTCGTCTATC	AGGACAGGACCCAGACAATG
cFos	TACTACCATTCCCCAGCCGA	GCTGTCACCGTGGGGATAAA
FosB	GTGAGAGATTTGCCAGGGTC	AGAGAGAAGCCGTCAGGTTG
ΔFosB	AGGCAGAGCTGGAGTCGGAGAT	GCCGAGGACTTGAACTTCACTCG
Gria1	CTGTGAATCAGAACGCCTCA	TCACTTGTCCTCCACTGCTG
Grin1	ACTCCCAACGACCACTTCAC	GTAGACGCGCATCATCTCAA
Homer1a	CTGACCAGTACCCCTTCACAG	TGTGTCACATCGGGTGTTCTC
Npas4	TATGGACTGCTACACCCCGA	GGCTTGAAGTCTCACCACCA
Nr4a1	AAAGTTGGGGGAGTGTGCTA	TGAGCTTGAATACAGGGCATCT
Ppia	CAAATGCTGGACCAAACACAAACG	GTTCATGCCTTCTTTCACCTTCCC
Rpl38	AGGATGCCAAGTCTGTCAAGA	TCCTTGTCTGTGATAACCAGGG
Rxra-1	CTGCCCATCCCTCAGGAAAT	TTGCAGCCCTCACAACTGTAT
Rxra-2	TGCAAGGGCTTCTTCAAGAG	TGGTGGACTCCACCTCGTTC
Tbp	CCCCACAACTCTTCCATTCT	GCAGGAGTGATAGGGGTCAT
Zif268	CTGACCAACGAGAAGCCCAA	TCCCAAGTAGGTCACGGTCT

Table S4. List of RT-qPCR primers. *(related to Figures 2, S2 and S3)*

Target	Company	Reference	Species	Dilution	RRID
ARC	Santa Cruz	sc-17839	Mouse monoclonal	2 µg/ml	AB_626696
pCREB	Cell Signaling Technologies	9198S	Rabbit monoclonal	1:1000	AB_2561044
pERK	Cell Signaling Technologies	4370S	Rabbit monoclonal	1:1000	AB_2315112
GluN2B	EMD Millipore	06-600	Rabbit polyclonal	1 µg/ml	AB_310193
PSD95	Abcam	ab18258	Rabbit polyclonal	1 µg/ml	AB_444362
p65/RELA	Invitrogen	436700	Mouse monoclonal	0.5 µg/ml	AB_2532217
TBP	Abcam	ab63766	Rabbit polyclonal	1 µg/ml	AB_1281140
RXRa	Abcam	ab125001	Rabbit monoclonal	0.12 µg/ml	AB_1097563
Actin	MP Biomedicals	691002	Mouse monoclonal	1:50000	AB_2335304

Table S5. List of antibodies and usage details. *(related to Figures 2, S2 and S3)*